



Particle Size Tailoring of Quercetin Nanosuspensions by Wet Media Milling Technique: A Study on Processing and Formulation Parameters

Pegah Cheshmehnoor¹, Noushin Bolourchian ¹, Erfan Abdollahizad¹, Arash Derakhshi¹, Simin Dadashzadeh ¹ and Azadeh Haeri^{1,2,*}

¹Department of Pharmaceutics and Pharmaceutical Nanotechnology, School of Pharmacy, Shahid Beheshti University of Medical Sciences, Tehran, Iran

²Protein Technology Research Center, Shahid Beheshti University, Tehran, Iran

*Corresponding author: Protein Technology Research Center, Shahid Beheshti University, Tehran, Iran. Email: a_haeri@sbmu.ac.ir

Received 2022 August 09; Revised 2022 December 03; Accepted 2022 December 10.

Abstract

Background: A large number of new substances have insufficient biopharmaceutical properties for oral administration caused by their slow dissolution rate and poor solubility.

Objective: The purpose of our experiment was to improve the physicochemical properties of a hydrophobic drug, quercetin, by the nanomilling approach.

Methods: Quercetin nanosuspensions were prepared using a wet-milling method followed by lyophilization. Stabilizer type and ratio, drug content, milling time, and bead size were identified as critical variables, and their impacts on quercetin particle size were assessed. The optimized nanocrystal was characterized by its morphology, crystallinity, molecular interactions, saturation solubility, and dissolution properties.

Results: At optimized process conditions of milling at 500 rpm for 18 cycles of grinding with 0.3 - 0.4 mm zirconium oxide beads, minimum particle size, and PDI values were 281.21 nm and 0.22, respectively. Nanocrystals showed rod-like nanostructures, and XRD scans confirmed a decrease in drug crystallinity. The optimized formulation showed increased solubility and dissolution rate, as well as good physical stability.

Conclusions: Particle size reduction by media milling technique was an efficient method for the solubility enhancement of hydrophobic drugs.

Keywords: Nanosuspensions, Quercetin, Wet Milling, Processing Parameters, Formulation Parameters

1. Background

A large number of new substances have insufficient biopharmaceutical properties for oral administration caused by their slow dissolution rate and poor solubility. Different approaches have been made to improve the water solubility of these cargoes (1-3). Particle size reduction is one of the promising formulation approaches to improve the oral bioavailability of poorly soluble drugs (4).

Nanosuspension is a promising drug delivery system for poorly soluble drugs (5). Nanosuspensions are dispersions of nanoparticles in liquid media, which are stabilized by surfactants, polymers, or a mixture of both (6). The main advantages of nanosuspensions for oral administration are enhanced dissolution rate and saturation solubility, improved adhesion to biological surfaces, and in-

creased patient compliance (7, 8).

Nanosuspensions can be prepared by two basic methods: Fracturing drug crystals into nanoparticles (top-down methods) or building up crystals from dissolved particles via precipitation techniques (bottom-up methods) (9). The top-down methods comprise high-energy processes such as media milling or high-pressure homogenization (HPH), which are industrially more feasible than other approaches (10).

Quercetin is a promising flavonoid that exerts anti-infective, anti-allergic, gastroprotective, anti-oxidant, anti-tumor, anti-diabetic, and anti-inflammatory effects (11). Quercetin has a typical flavonoid structure and contains five hydroxyl groups (12). Quercetin molecules are tightly packed, increasing intermolecular force (13). The aqueous solubility of quercetin varies from 1.5 to 12.5 mg/L de-

pending upon the pH level, which limits its oral absorption. Moreover, the octanol-water partition coefficient of quercetin was reported to be 1.8 ± 0.3 (14); all these factors result in the low oral bioavailability of quercetin which is about 17% in mice (15, 16).

This study aimed to develop quercetin nanosuspensions to improve their solubility and oral bioavailability. At present, several preparation techniques have been applied to fabricate quercetin nanosuspensions, such as HPH (17, 18), solvent replacement (19), precipitation (20), and wet media milling (21). Kakran et al. studied three different fabrication methods for preparing quercetin nanocrystals, including HPH, cavi-precipitation, and bead milling (22). Considering the same formulation composition, bead milling produced the smallest particle size (276 nm), followed by HPH and precipitation. In another experiment, Lai and colleagues developed quercetin nanocrystals in the 326 - 474 nm range for dermal delivery using the wet milling technique (21). The mentioned studies mainly focused on the influence of milling time, bead size, and drug concentration. To the best of our knowledge, there has been no research investigating the effect of critical formulation parameters (the drug-to-stabilizer weight ratio and the stabilizer type) on quercetin nanosuspensions prepared by milling technology.

2. Objectives

In this study, quercetin nanosuspensions were fabricated by wet media milling. Moreover, the influence of formulation parameters (ratio of drug to the stabilizer, drug content, and stabilizer type) and process variables (milling time and bead size) on nanosuspension properties were evaluated during media milling. To enhance long-term stability, the freshly prepared nanosuspensions were lyophilized using various cryoprotectants. The formulations were optimized and fully characterized.

3. Methods

3.1. Materials

Quercetin, fructose, lactose, mannitol, sucrose, polysorbate 80 (Tween 80), Poloxamer 188 (F68), Poloxamer 407 (F127), and D- α -Tocopherol polyethylene glycol 1000 succinate (TPGS) were purchased from Merck/Sigma-Aldrich (Germany). Labrasol was kindly provided by Gattefossé (France).

3.2. Preparation of Nanosuspensions by Wet Media Milling Method

Nanosuspensions were fabricated by wet media milling technique using a planetary ball mill (NARYA-MPM-2*250H, Iran). First, the stabilizer was dissolved in 5 mL of deionized water. Quercetin powder was then dispersed in the aqueous solution of stabilizer and kept under mechanical stirring to ensure sufficient wetting. The suspensions were transferred to a milling chamber containing milling pearls (30 g, zirconium oxide beads with diameters of 0.6 - 0.8 mm or 0.3 - 0.4 mm). The milling process was performed at 500 rpm for various cycles, each consisting of 5 min of milling followed by a 5 min break. The sieving was used to separate the obtained nanosuspensions.

3.3. Determination of Particle Size, Polydispersity, and Zeta Potential

The particle size, zeta potential, and polydispersity index (PDI) were determined by a Zetasizer Nano ZS instrument after appropriate dilution of samples with deionized water.

3.4. Lyophilization of Nanosuspensions

Volumes of suspensions equivalent to 1 mg of drug substance were transferred into glass vials. Amounts of different cryoprotectants (mannitol, sucrose, fructose, and lactose) corresponding to 200% and 400% w/w relative to the drug content were added to the nanosuspension. Samples were frozen at -80°C for 24 h; then, the frozen samples were dried using an LDplus (Germany) freeze-dryer.

3.5. Reconstitution of Freeze-dried Powder

Nanocrystals were suspended in distilled water, and the dispersion was shaken. Then, the particle size and PDI were determined, and the redispersibility index (RDI) (Equation 1) was calculated by the following equation:

$$RDI = \left[\frac{D}{D_0} \right] \times 100\% \quad (1)$$

Where D_0 and D were the mean particle size of fresh nanosuspensions and redispersed nanocrystals, respectively.

3.6. Morphology Observations

The morphology of the quercetin particles was examined by scanning electron microscopy (SEM) and atomic force microscopy (AFM). The surface morphologies of unprocessed materials and freeze-dried particles were evaluated by SEM. Samples were placed on a brass stub and coated with a gold sputtering coater before analysis. For

AFM observation, particles were observed in contact mode. The diluted samples were deposited onto the mica plate and dried at ambient temperature.

3.7. FTIR Analysis

The molecular structures of unprocessed materials, physical mixtures, and nanocrystals were studied using FTIR spectroscopy. Samples were pressed into KBr discs, and the compressed discs were scanned over the range of 400 - 4000 cm^{-1} .

3.8. X-ray Diffraction Analysis

X-ray powder diffraction (XRD) spectra of coarse quercetin powders, stabilizers, cryoprotectants, physical mixtures, and freeze-dried nanosuspensions were recorded using an X-ray diffractometer with Cu $K\alpha$ radiation operating at a voltage of 40 kV and a current of 30 mA.

3.9. In Vitro Drug Dissolution Studies

Dissolution profiles were investigated using a paddle (USP II) apparatus at $37 \pm 0.5^\circ\text{C}$ in 200 mL of simulated gastric fluid (pH 1.2) and phosphate buffer (pH 6.8) containing 0.2% Tween 80 at 100 rpm. Accurately weighed samples equivalent to 5 mg of quercetin were directly added to the dissolution medium. 10 mL aliquots were withdrawn at certain time intervals, filtered by 0.22 μm filters, replaced with the same volume of fresh medium, and analyzed for the content of dissolved quercetin by UV-Visible spectrophotometer. Sampling was performed for up to 120 min and 240 min at pH 1.2 and pH 6.8, respectively.

3.10. Solubility Measurements

The saturation solubility was determined by placing samples (raw quercetin, physical mixture, and nanocrystals) containing the same amount of drug (3 mg) in capped vials containing 3 mL deionized water. Samples were shaken at 300 rpm for 12 h at 25°C . When equilibrium was reached, samples were centrifuged, and the UV absorbance of the supernatant was determined at 370 nm after appropriate dilution with distilled water containing 10% (v/v) methanol.

3.11. Stability Study

At the pre-determined time points, the freeze-dried powders of quercetin nanosuspensions were resuspended. The stability of the optimized formulations was studied at -20°C for up to 4 months by the measurements of the changes in particle size and distribution, zeta potential, and quercetin content.

3.12. Statistical Analysis of Data

Statistical analyses were carried out using SPSS 22.0. The unpaired *t*-test was used to compare the two mean values, while multiple mean values were compared using the one-way analysis of variance (ANOVA). A *P* value of < 0.05 was considered statistically significant.

4. Results

4.1. Preparation of Quercetin Nanosuspensions by Wet Media Milling Technology

In this study, quercetin nanosuspensions were prepared by the wet milling technique using a planetary ball mill. The impact of various formulation and process parameters on the mean particle size and PDI of quercetin nanosuspensions is summarized in Table 1. Various stabilizers, including F68, F127, Tween 80, TPGS, and Labrasol were used to develop stable quercetin nanosuspensions. As shown in Table 1, by changing the type of the stabilizer and keeping other parameters constant, the mean particle size and PDI of the nanoformulations (F1-F5) were in the range of 401.58-611.38 nm and 0.44 - 0.56, respectively. The smallest average particle size and PDI were achieved by the F68 stabilizer (F4) ($P < 0.05$).

Two different size ranges (0.6 - 0.8 mm and 0.3-0.4 mm) of yttrium-stabilized zirconia milling beads were used as the grinding media. After nanomilling for about 30 min, a smaller particle size (334.82 nm vs. 401.58 nm) was obtained by 0.3 - 0.4 mm beads ($P < 0.05$) as they provided a greater surface area for milling. Thus, smaller beads (0.3 - 0.4 mm) were selected for further nanomilling studies.

To investigate the amount of stabilizer, two different drugs to stabilizer ratios were tried on a weight basis (2:1 and 4:1). Although the particle size decreased at higher stabilizer concentration (F6), no significant differences were observed ($P > 0.05$); hence the 4: 1 ratio was selected for further experiments as using smaller amounts of surfactant was preferred.

Increasing the drug content from 2.5 to 5% at a constant drug-to-stabilizer ratio (4: 1) improved the milling efficiency. The Z-average decreased from 360.74 nm to 344.65 nm, concurrent with decreasing the PDI from 0.41 to 0.39. However, when the drug concentration was further increased to 10%, the particle size was found to be slightly increased ($P > 0.05$). Therefore, the drug content of 5% was selected for further experiments due to lower quercetin consumption during the experiments.

Milling duration significantly affected the mean particle size and PDI of quercetin nanosuspensions. Particle size in the nanometer range was achieved within the first 30 min of milling (F1-F9). As the milling time increased to

Table 1. Effect of Various Process and Formulation Parameters on the Mean Particle Size and PDI of Wet-milled Nanosuspensions (mean \pm SEM, n = 3)

Formulation	Stabilizer Type	Bead Size (mm)	Drug: Stabilizer Ratio	Drug Load%	Milling Time (min)	Size (nm)	PDI
F1	Tween 80	0.6 - 0.8	2	2.5	30	537.42 \pm 37.06	0.52 \pm 0.04
F2	Labrasol®	0.6 - 0.8	2	2.5	30	611.38 \pm 33.17	0.56 \pm 0.01
F3	F127	0.6 - 0.8	2	2.5	30	472.10 \pm 22.29	0.49 \pm 0.03
F4	F68	0.6 - 0.8	2	2.5	30	401.58 \pm 9.77	0.44 \pm 0.02
F5	TPGS	0.6 - 0.8	2	2.5	30	423.62 \pm 32.59	0.46 \pm 0.02
F6	F68	0.3 - 0.4	2	2.5	30	334.82 \pm 9.08	0.41 \pm 0.02
F7	F68	0.3 - 0.4	4	2.5	30	360.74 \pm 14.63	0.41 \pm 0.01
F8	F68	0.3 - 0.4	4	5	30	344.65 \pm 8.50	0.39 \pm 0.01
F9	F68	0.3 - 0.4	4	10	30	366.97 \pm 1.98	0.36 \pm 0.01
F10	F68	0.3 - 0.4	4	5	60	346.86 \pm 18.43	0.36 \pm 0.01
F11	F68	0.3 - 0.4	4	5	90	281.21 \pm 4.26	0.22 \pm 0.02
F12	F68	0.3 - 0.4	4	5	120	318.36 \pm 11.89	0.25 \pm 0.01

90 min, the mean particle size and PDI decreased to 281.21 nm and 0.22, respectively. Furthermore, a slight increase in particle size and PDI ($P > 0.05$) occurred when the milling time was prolonged to more than 90 min (F12). Thus, 90 min was found to be the optimum milling time for the preparation of the smallest quercetin nanoparticles (F11).

4.2. Lyophilization of Quercetin Nanosuspensions

Lyophilization of the optimized nanosuspension (F11) was performed to transform the aqueous nanosuspensions into a stable state, keeping the initial particle size and PDI after reconstitution. Table 2 depicts the effect of the type and concentration of cryoprotectants on the mean size and PDI of the quercetin particles immediately after reconstituting the nanocrystals. Quercetin nanocrystals in the presence of fructose were found to produce better RDI than other cryoprotectants. Increasing the cryoprotectant concentration to 400% w/w slightly decreased the mean particle size and PDI of the redispersed nanosuspensions ($P > 0.05$). After the dispersion of bare nanocrystals, a much higher increase in particle size and the RDI value of 147% were observed (Table 2).

4.3. Physicochemical Characterization of Quercetin Nanoformulations

Figures 1A and 1B show the SEM micrographs of the unprocessed quercetin powder and optimized nanocrystals under different magnifications. The SEM photomicrographs reveal the irregular and rough morphology of pure quercetin compared to the relatively rod-shaped and smooth morphology of nanocrystals. AFM topographic and 3D images of redispersed nanosuspensions were also

scanned in an area of $2 \mu\text{m} \times 2 \mu\text{m}$. From Figure 1C, it is evident that the morphology of the wet-milled nanoparticles is non-spherical shaped and well distributed with a diameter range of $< 1 \mu\text{m}$.

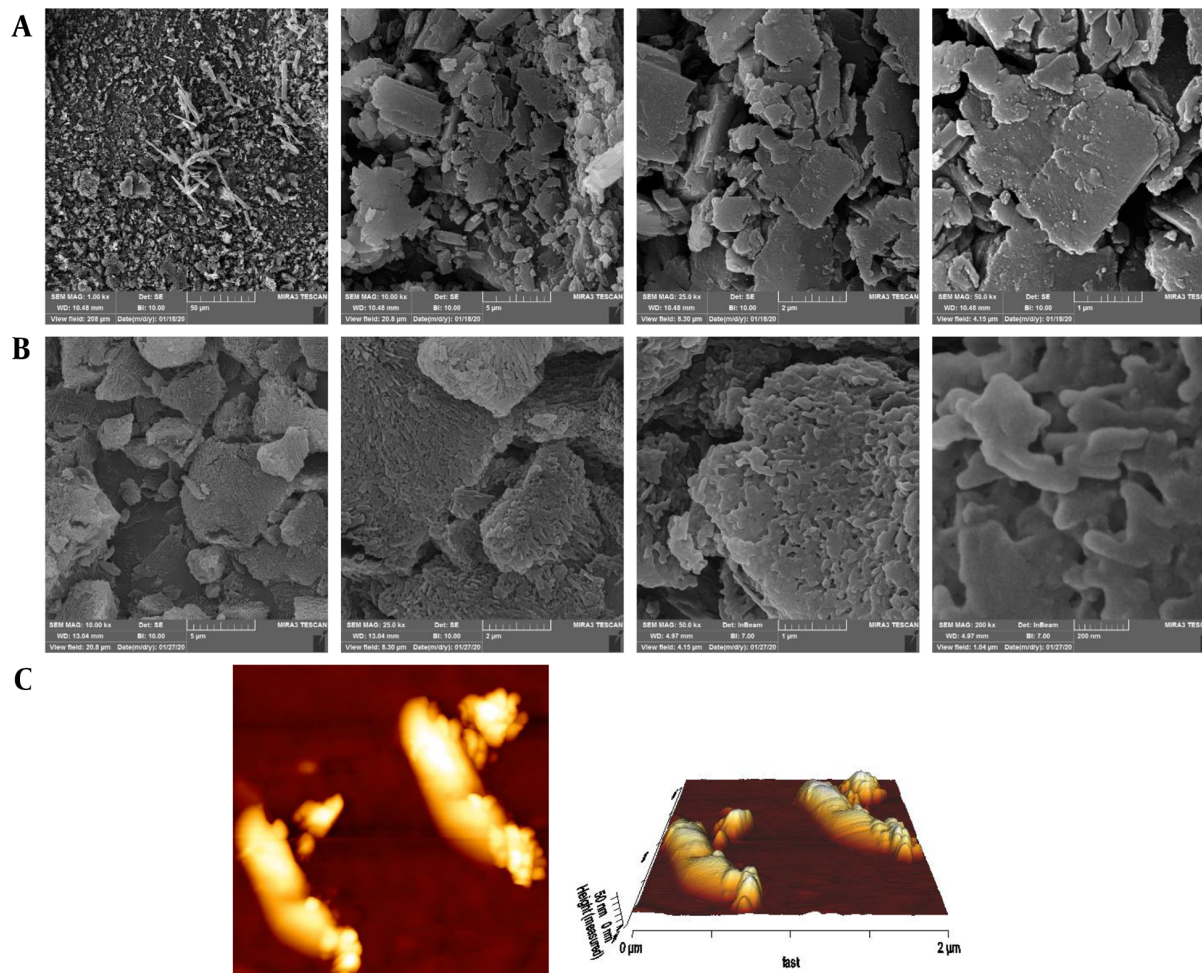
The FTIR spectrum (Figure 2A) of pure quercetin exhibited characteristic peaks at 3406 cm^{-1} corresponding to O-H phenolic stretching, two intense absorption bands at 1668 cm^{-1} and 1608 cm^{-1} representing the stretching vibration of carbonyl (C=O) group, 1558 cm^{-1} and 1520 cm^{-1} assigned to the aromatic ring, 1168 cm^{-1} and 1319 cm^{-1} due to C-O-C stretching and 863 cm^{-1} corresponding to C-H bending vibrations. In the case of F68, the absorption bands due to stretching of O-H, C-O, and C-H groups appeared at 3490 cm^{-1} , 1109 cm^{-1} , and 2885 cm^{-1} , respectively. The spectrum of fructose displayed a characteristic peak at 3523 cm^{-1} attributed to O-H stretching. Stretching vibrations of the methylene group were detected around 2900 cm^{-1} , and other absorption bands at 1095 cm^{-1} , 1078 cm^{-1} , and 1053 cm^{-1} were assigned to C-O stretching vibrations. FTIR spectrum of both physical mixtures showed characteristic peaks of pure quercetin, indicating that the interaction between the API and stabilizers was negligible.

Likewise, in the spectrum of the wet-milled nanocrystal, the characteristic peaks of quercetin and F68 were present at almost the same positions suggesting the absence of any chemical interaction within the milling process.

The XRD pattern of quercetin displayed sharp and intense peaks at 2θ scattering angles of 10.75° , 12.44° , and 27.38° , reflecting the crystalline nature of quercetin in native form (Figure 2B). Only two prominent peaks at 2θ of 19.16° and 23.39° were observed in the F68 spectrum. The spectrum of the quercetin: F68 physical mixture was sim-

Table 2. The Influence of Cryoprotectant Type and Concentration on the Mean Particle Size, PDI, and RDI of Reconstituted Samples of Lyophilized Quercetin Nanosuspensions (Mean \pm SEM, n = 3)

Variables	Fresh Nanosuspension	Mannitol		Fructose		Lactose		Sucrose		No Cryoprotectant
		2	4	2	4	2	4	2	4	
Size	280.50 \pm 6.81	274.04 \pm 34.28	260.47 \pm 16.06	253.39 \pm 10.04	265.20 \pm 12.77	280.93 \pm 11.75	272.16 \pm 10.95	258.02 \pm 18.13	254.88 \pm 14.16	411.47 \pm 23.83
PDI	0.24 \pm 0.02	0.33 \pm 0.02	0.29 \pm 0.02	0.26 \pm 0.01	0.24 \pm 0.01	0.28 \pm 0.02	0.26 \pm 0.02	0.28 \pm 0.02	0.28 \pm 0.02	0.46 \pm 0.06
RDI%	-	97.7	92.9	90.3	94.5	100.2	97.0	92.0	90.9	146.7

**Figure 1.** SEM and AFM analyses of quercetin particles. SEM images of (A) unmilled quercetin and (B) freeze-dried nanosuspensions. (C) 2D and 3D AFM images of redispersed nanocrystals.

ilar to pure quercetin; no diffraction peaks of F68 were detected. The XRD results indicated that the crystalline state of the cargo was present in the nanocrystal, as evident by the presence of the predominant peaks of crystalline quercetin (at 10.72°, 12.46°, and 27.40°) with a slight transition of peak intensities.

The *in vitro* dissolution of nanocrystals was carried out in gastric juice (pH=1.2) (Figure 3A) and intestinal fluid (pH = 6.8) (Figure 3B) to simulate their performance in the di-

gestive tract. Freeze-dried quercetin nanosuspension powders showed distinctly superior dissolution velocity compared to those of the coarse powder and physical mixture. As seen in Figure 3A, 63.55% of the drug was dissolved from quercetin nanocrystal in an acidic solution after 2 h. In contrast to this, the crude quercetin powder and physical mixture were dissolved up to 47.71% and 49.08%, respectively. A similar dissolution behavior was also observed in phosphate buffer pH 6.8 (Figure 3B). Quercetin powder and

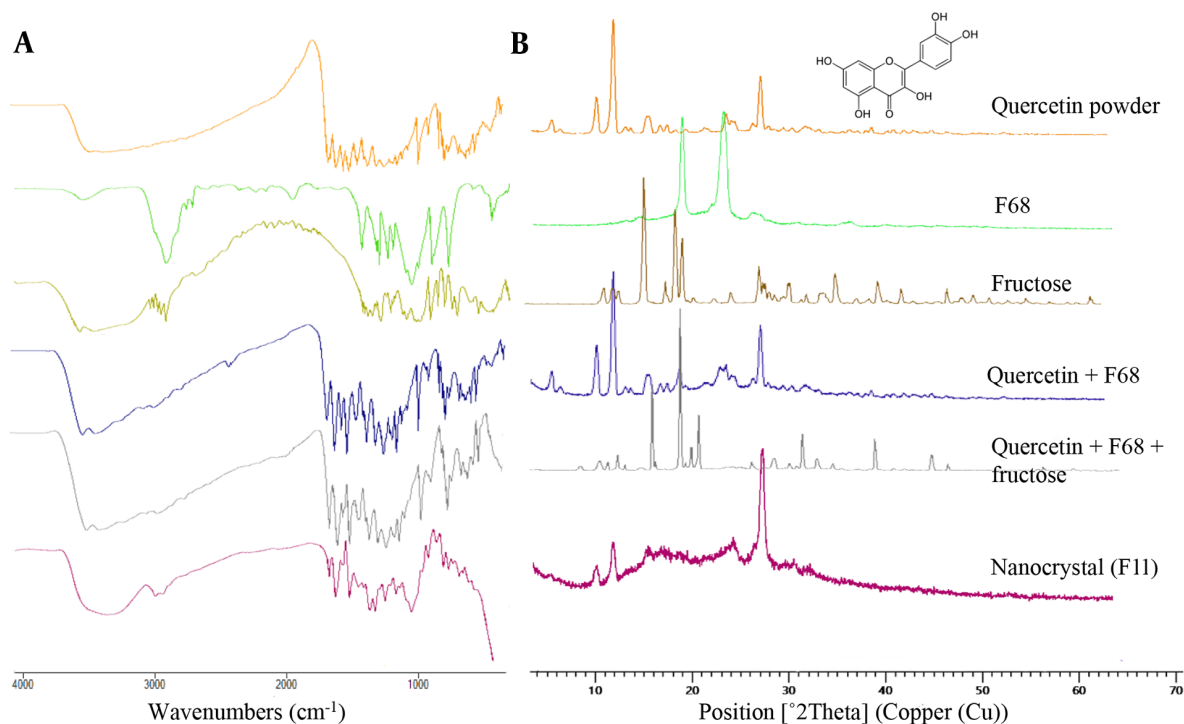


Figure 2. (A) FTIR and (B) XRD spectra for unprocessed quercetin, F68, fructose, physical mixtures, and wet-milled nanocrystals.

physical mixture showed poor dissolution characteristics. Only 51.64% and 50.74% were released within 4 h, respectively, while it was almost 65.20% in the case of nanocrystals after the same period. The solubility values of pure quercetin and the physical mixture were 1.58 ± 0.13 and 1.31 ± 0.09 $\mu\text{g/mL}$, respectively. The freeze-dried nanosuspension showed maximum saturation solubility (15.96 ± 1.16 $\mu\text{g/mL}$). In general, milling for 90 min resulted in the formation of nanoparticles with a 10-fold increase in saturation solubility of the drug (Figure 3C).

The monitoring of particle size, PDI, zeta potential, and drug content values was conducted upon storage for four months at -20°C . Figure 4 indicates that the optimum formulation retained similar particle size and PDI after four months. Although the zeta potential fluctuated on a time basis, the value varied between -16.7 to -23.2 mV, and the quercetin content (%) maintained steadily at a range of 96.2 - 100.1%, demonstrating acceptable physical and chemical stability.

5. Discussion

Nanosuspensions have received considerable attention in the drug delivery field for solubility and dissolution

rate enhancement of hydrophobic drugs (23). Nanosuspensions can be fabricated by top-down and bottom-up approaches. Wet media milling and HPH are top-down approaches for preparing nanocrystals (24). Nanomilling is a process in which particle size reduction is obtained by the impact of the milling medium with the drug particles. The robustness and reproducibility of nanosuspension preparation are governed by different formulations and operating factors (25).

In this work, the effect of different stabilizers was studied on the particle size and PDI of quercetin nanosuspensions. The initial screening revealed that F68 was the most appropriate one, followed by TPGS and F127 (Table 1). There was no significant difference in the mean particle size of F3, F4, and F5 formulations stabilized by the stabilizers as mentioned above ($P > 0.05$). Comparing the chemical structure of stabilizers, it can be noted that Pluronics are tri-block co-polymers consisting of two hydrophilic poly (ethylene oxide) (PEO) terminals with central hydrophobic poly (propylene oxide) (PPO) block (26). F127 and F68 have the same basic structure but differ in the length of PEO and PPO groups. The slightly improved performance of F68 compared to F127 could be ascribed to its lower molecular weight, leading to a less restricted adsorption process and

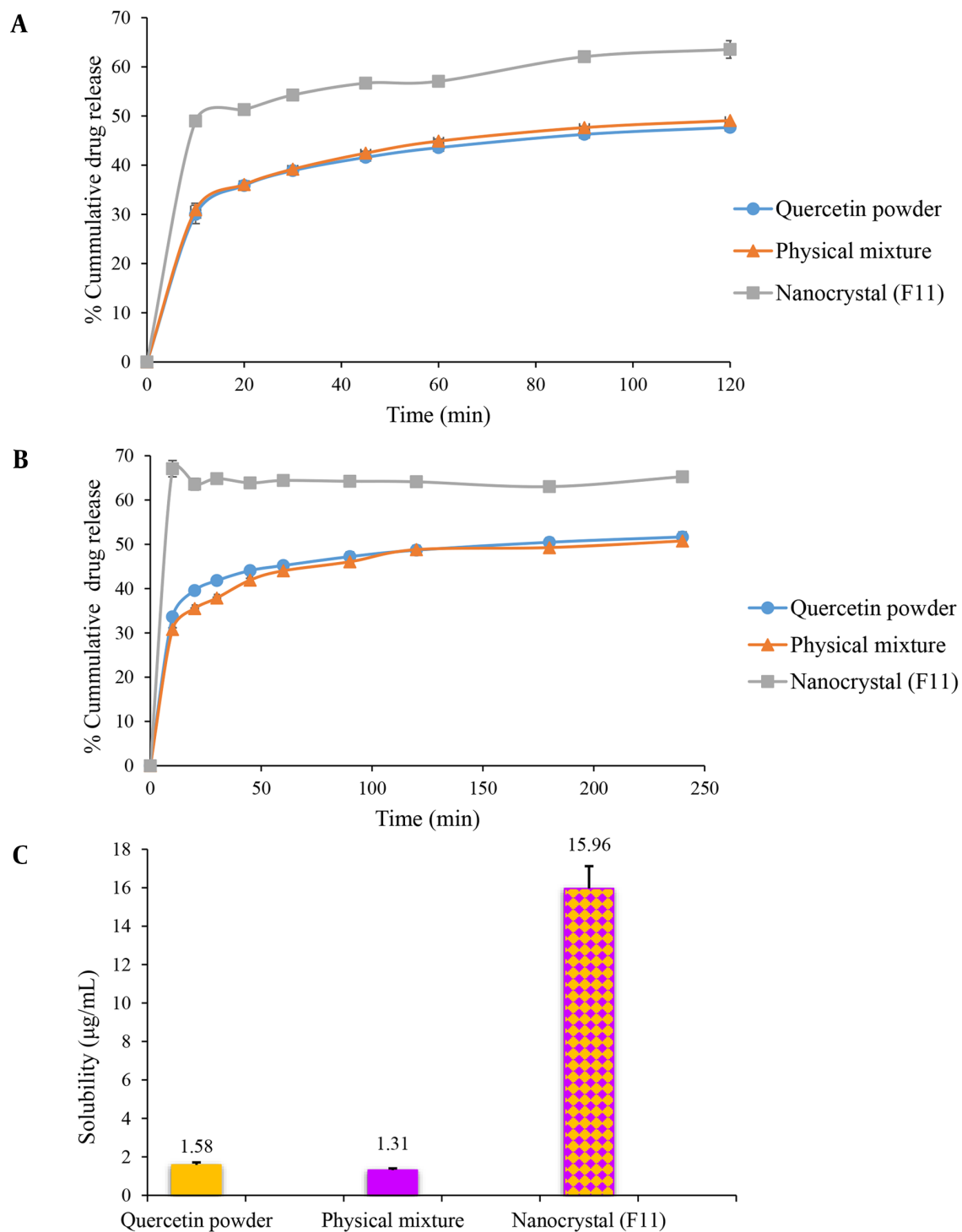


Figure 3. In vitro release profile of quercetin from quercetin powder, physical mixture, and the optimized nanocrystal in gastric (pH = 1.2) (A) and intestinal fluids (pH = 6.8) (B). (C) The saturation solubility of quercetin powder, physical mixture, and the optimized nanocrystal in distilled water. Data are presented as mean \pm SEM; n = 3.

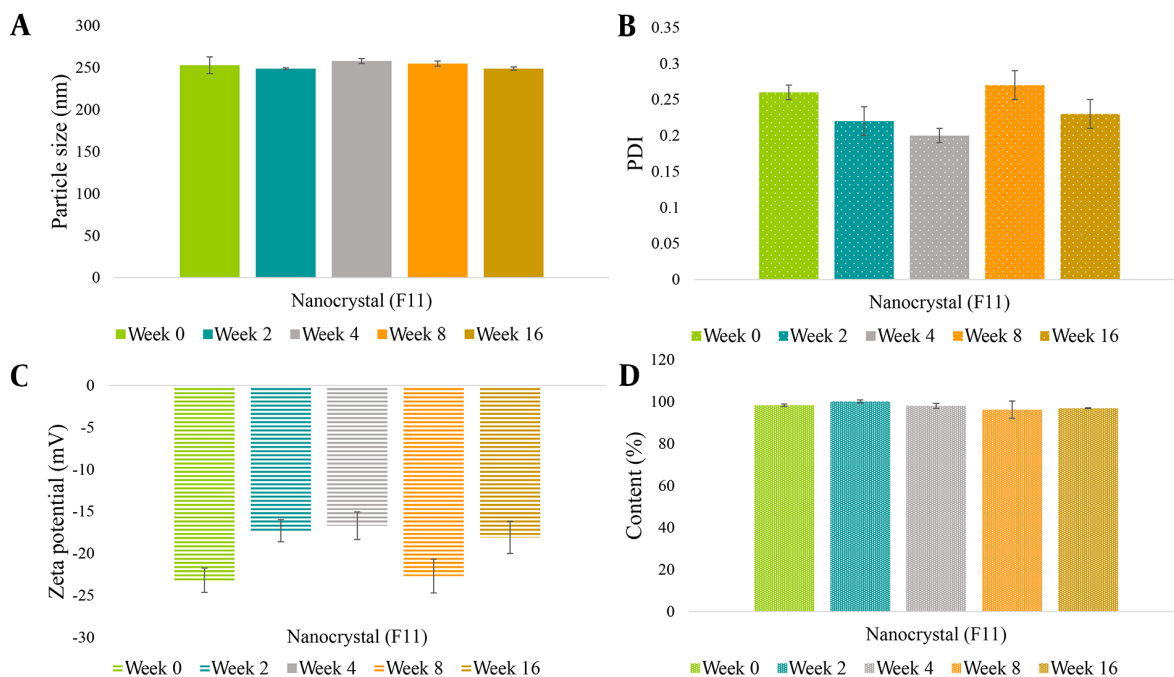


Figure 4. (A) Mean particle size, (B) PDI, (C) zeta potential, and (D) quercetin content changes of reconstituted nanosuspensions during storage at -20°C . Data are presented as mean \pm SEM; n = 3.

a faster diffusion (27). Additionally, TPGS is composed of only one hydrophilic polar head and a hydrophobic alkyl tail (28) and results in larger particle sizes than formulations stabilized by the polymers.

The intensity of grinding energy affects the performance of the wet media milling, and proper selection of the bead size plays a major role in the breakage kinetics (29). Smaller beads (0.3-0.4 mm) resulted in finer nanoparticles at the same milling time (Table 1). The possible reason is that the number of contact points is increased exponentially with a reduction in the size of milling beads, resulting in better grinding efficiency and, therefore, smaller particles.

According to the theory, the concentration of stabilizers should be sufficient to cover the entire surface of drug particles to provide a barrier against aggregation (30). The particle size and PDI of nanosuspensions at two drugs: Stabilizer ratios (4:1 and 2:1) were investigated (F6 vs. F7). Results indicated that by increasing the concentration of F68, the particle size slightly decreased ($P > 0.05$). The higher stabilizer concentration allows the adsorption of more stabilizer molecules onto the surface of drug particles leading to better steric hindrance between the nanoparticles and particle size reduction (31).

Regarding the effect of different drug loading, an in-

crease in the drug loading from 2.5% to 5% led to a slight decrease in particle size ($P > 0.05$). This result could be attributed to additional attrition between the particles by higher solid content (32). Moreover, with increasing drug amounts, more particles are trapped in the active grinding region between the milling beads, leading to improved milling efficiency. The latter assumption is in line with the findings of Cerdeira et al. working on miconazole nanosuspensions (33). However, as shown in Table 1, a further increase in drug loading to 10%, yielded a negative impact on the mean particle size. This was probably due to the insufficient collision between the drug particles and milling beads by increasing the drug content above an optimum level.

The final studied process variable was milling time. The mean size and PDI of nanoparticles decreased steadily with an increase in milling time. As reported by Alshora et al., this result could be attributed to the increased probability of collision between drug particles and milling beads (34). Besides, increasing milling time provides sufficient time for the adsorption of the stabilizers onto the drug particles (35). However, the particle size of quercetin was enlarged by a further increase in milling time beyond an optimum level (90 min), possibly, due to increased collision and aggregation between the newly generated particles. A

similar trend has been reported by Yuan and coworkers, who investigated the effect of milling time on the mean particle size of nitrofurazone nanosuspensions (36).

Lyophilization is a common drying method applied to stabilize nanosuspensions and increase their shelf life (37). Cryoprotectants are used during the solidification step to prevent the irreversible aggregation of nanoparticles. Adding sugars or sugar alcohols as cryoprotectants prevents nanocrystalline aggregation during the drying processes (38). The mean particle sizes of the reconstituted powders with cryoprotective agents were smaller than that of the control powders (Table 2). This is because cryoprotectants protect the nanosuspensions from freezing damage caused by ice formation (39). A concentration-dependent cryoprotection and a slight decrease ($P > 0.05$) in particle size at higher concentrations of cryoprotectants were observed, which could be due to better protection effects.

FTIR analysis was performed to gain insight into possible molecular interactions between the drug and stabilizer. As depicted in Figure 2A, the spectrum of quercetin presented absorption peaks of hydroxyl, carbonyl, and aromatic groups, which are consistent with the values reported in the literature (40, 41). The nanocrystal spectra appeared as the summation of quercetin, F68, and fructose, indicating that no chemical interaction occurred between the drug and stabilizer. The peak broadening at 3300-3500 cm^{-1} may be attributed to the hydrogen bonding between quercetin and fructose hydroxyl groups.

XRD analysis was carried out to elucidate the physical structure of the drug in the nanocrystals. Based on the diffractograms presented in Figure 2B, quercetin powder revealed its crystalline nature as proved by well-defined predominant diffraction peaks in the 2θ range of $10^\circ - 30^\circ$ (42). Changes in the crystallinity of quercetin were qualitatively assessed based on the sharpness of the main characteristic peaks. The pattern of the wet-milled nanocrystal demonstrated differences in the intensity of peaks compared to the pure quercetin, which probably represents a slight reduction in crystallinity or partial amorphization of quercetin by nanomilling. These observations can explain the higher solubility of nanocrystals as compared to the unprocessed powder (43).

Dissolution velocities of the nanocrystals were distinctly superior compared to the quercetin coarse powders and physical mixtures (Figures 3A and 3B). The rate of drug dissolution could be described by the Noyes-Whitney equation (Equation 2), according to which the dissolution velocity (dc/dt) is proportional to the surface area (A) available for dissolution (44).

$$\frac{dc}{dt} = \frac{DA(C_s - C_t)}{h} \quad (2)$$

In the equation, D is the diffusion coefficient, C_s is the saturation solubility, C_t is the bulk concentration, and h is the thickness of the diffusion layer. Particle size reduction down to the nanometric level increases the effective surface area.

Lai et al. reported a slight increase in the dissolution rate of physical mixtures compared to the bulk diclofenac powder due to the solubilization effect of stabilizers (45). Contrary to expectations, we found that adding an equivalent amount of F68 present in nanoformulations to the quercetin powder could not improve the quercetin dissolution rate, probably due to insufficient quantity.

To improve long-term storage, we freeze-dried nanosuspensions shortly after milling to prepare solid formulations. The size of nanocrystals varied less than 10% during the stability test, suggesting desirable storage stability of the lyophilized form (Figure 4). There was a negligible change in the quercetin content of the nanocrystals after four months of storage.

5.1. Conclusions

In the present study, quercetin nanosuspensions with mean diameters of less than 300 nm and uniform size distributions were prepared using the wet media milling technique with a careful selection of formulation and process parameters. Stabilizer type, drug: Stabilizer ratio, drug content, bead size, and milling time were identified as key factors throughout the experiment. Nanosuspensions were subsequently solidified to ensure their long-term stability. Based on these findings, wet media milling is a promising strategy for improving the dissolution rate and thus enhancing the oral bioavailability of quercetin and other poorly water-soluble drugs.

Footnotes

Authors' Contribution: Conceptualization, A.H., S.D., and N.B.; Methodology, A.H. and P.C.; Data analysis, P.C., A.D., E.A., A.H., S.D., and N.B.; Investigation, P.C. A.D., E.A., and A.H.; Initial draft preparation, P.C.; Review and editing, A.H., S.D., and N.B.; Supervision, A.H., S.D., and N.B.; All authors have read and agreed to the published version of the manuscript.

Conflict of Interests: This work was supported by Shahid Beheshti University of Medical Sciences under Grant number 17430. Azadeh Haeri is a member of the Editorial Board of IJPR. The authors declare no conflicts of interest.

Data Reproducibility: The dataset presented in the study is available on request from the corresponding author during submission or after publication.

Ethical Approval: <https://ethics.research.ac.ir/EthicsProposalView.php?id=66674>

Funding/Support: Present study is a part of PharmD thesis of the first author, Pegah Cheshmehnoor and supported by Shahid Beheshti University of Medical Sciences under Grant number 17430.

References

- Kawabata Y, Wada K, Nakatani M, Yamada S, Onoue S. Formulation design for poorly water-soluble drugs based on biopharmaceutics classification system: basic approaches and practical applications. *Int J Pharm.* 2011;**420**(1):1-10. [PubMed ID: 21884771]. <https://doi.org/10.1016/j.ijpharm.2011.08.032>.
- Babadi D, Dadashzadeh S, Osouli M, Daryabari MS, Haeri A. Nanof ormulation strategies for improving intestinal permeability of drugs: A more precise look at permeability assessment methods and pharmacokinetic properties changes. *J Control Release.* 2020;**321**:669-709. [PubMed ID: 32112856]. <https://doi.org/10.1016/j.jconrel.2020.02.041>.
- Alavi S, Akhlaghi S, Dadashzadeh S, Haeri A. Green Formulation of Triglyceride/Phospholipid-Based Nanocarriers as a Novel Vehicle for Oral Coenzyme Q10 Delivery. *J Food Sci.* 2019;**84**(9):2572-83. [PubMed ID: 31436862]. <https://doi.org/10.1111/1750-3841.14763>.
- Merisko-Liversidge E, Liversidge GG. Nanosizing for oral and parenteral drug delivery: a perspective on formulating poorly-water soluble compounds using wet media milling technology. *Adv Drug Deliv Rev.* 2011;**63**(6):427-40. [PubMed ID: 21223990]. <https://doi.org/10.1016/j.addr.2010.12.007>.
- Gao L, Liu G, Ma J, Wang X, Zhou L, Li X, et al. Application of drug nanocrystal technologies on oral drug delivery of poorly soluble drugs. *Pharm Res.* 2013;**30**(2):307-24. [PubMed ID: 23073665]. <https://doi.org/10.1007/s11095-012-0889-z>.
- Goke K, Lorenz T, Repanas A, Schneider F, Steiner D, Baumann K, et al. Novel strategies for the formulation and processing of poorly water-soluble drugs. *Eur J Pharm Biopharm.* 2018;**126**:40-56. [PubMed ID: 28532676]. <https://doi.org/10.1016/j.ejpb.2017.05.008>.
- Leone F, Cavalli R. Drug nanosuspensions: a ZIP tool between traditional and innovative pharmaceutical formulations. *Expert Opin Drug Deliv.* 2015;**12**(10):1607-25. [PubMed ID: 25960000]. <https://doi.org/10.1517/17425247.2015.1043886>.
- Shegokar R, Muller RH. Nanocrystals: industrially feasible multifunctional formulation technology for poorly soluble actives. *Int J Pharm.* 2010;**399**(1-2):129-39. [PubMed ID: 20674732]. <https://doi.org/10.1016/j.ijpharm.2010.07.044>.
- Liu Y, Xie P, Zhang D, Zhang Q. A mini review of nanosuspensions development. *J Drug Target.* 2012;**20**(3):209-23. [PubMed ID: 22192053]. <https://doi.org/10.3109/1061186X.2011.645161>.
- Alam MA, Al-Jenoobi FI, Al-Mohizea AM. Commercially bioavailable proprietary technologies and their marketed products. *Drug Discov Today.* 2013;**18**(19-20):936-49. [PubMed ID: 23707660]. <https://doi.org/10.1016/j.drudis.2013.05.007>.
- D'Andrea G. Quercetin: A flavonol with multifaceted therapeutic applications? *Fitoterapia.* 2015;**106**:256-71. [PubMed ID: 26393898]. <https://doi.org/10.1016/j.fitote.2015.09.018>.
- Wang W, Sun C, Mao L, Ma P, Liu F, Yang J, et al. The biological activities, chemical stability, metabolism and delivery systems of quercetin: A review. *Trends Food Sci Technol.* 2016;**56**:21-38. <https://doi.org/10.1016/j.tifs.2016.07.004>.
- Zhou Y, Suo W, Zhang X, Lv J, Liu Z, Liu R. Roles and mechanisms of quercetin on cardiac arrhythmia: A review. *Biomed Pharmacother.* 2022;**153**:113447. [PubMed ID: 36076562]. <https://doi.org/10.1016/j.biopha.2022.113447>.
- Guo Y, Bruno RS. Endogenous and exogenous mediators of quercetin bioavailability. *J Nutr Biochem.* 2015;**26**(3):201-10. [PubMed ID: 25468612]. <https://doi.org/10.1016/j.jnutbio.2014.10.008>.
- Shi GJ, Li Y, Cao QH, Wu HX, Tang XY, Gao XH, et al. In vitro and in vivo evidence that quercetin protects against diabetes and its complications: A systematic review of the literature. *Biomed Pharmacother.* 2019;**109**:1085-99. [PubMed ID: 30551359]. <https://doi.org/10.1016/j.biopha.2018.10.130>.
- Khurshed R, Singh SK, Wadhwa S, Gulati M, Awasthi A. Enhancing the potential preclinical and clinical benefits of quercetin through novel drug delivery systems. *Drug Discov Today.* 2020;**25**(1):209-22. [PubMed ID: 31707120]. <https://doi.org/10.1016/j.drudis.2019.11.001>.
- Karadag A, Ozcelik B, Huang Q. Quercetin nanosuspensions produced by high-pressure homogenization. *J Agric Food Chem.* 2014;**62**(8):1852-9. [PubMed ID: 24471519]. <https://doi.org/10.1021/jf404065p>.
- Sahoo NG, Kakran M, Shaal LA, Li L, Muller RH, Pal M, et al. Preparation and characterization of quercetin nanocrystals. *J Pharm Sci.* 2011;**100**(6):2379-90. [PubMed ID: 21491450]. <https://doi.org/10.1002/jps.22446>.
- Pessoa LZDS, Duarte JL, Ferreira RMDA, Oliveira AEMDFM, Cruz RAS, Faustino SMM, et al. Nanosuspension of quercetin: preparation, characterization and effects against *Aedes aegypti* larvae. *Rev Bras Farmacogn.* 2018;**28**(5):618-25. <https://doi.org/10.1016/j.bjpp.2018.07.003>.
- Gao L, Liu G, Wang X, Liu F, Xu Y, Ma J. Preparation of a chemically stable quercetin formulation using nanosuspension technology. *Int J Pharm.* 2011;**404**(1-2):231-7. [PubMed ID: 21093559]. <https://doi.org/10.1016/j.ijpharm.2010.11.009>.
- Manca ML, Lai F, Pireddu R, Valenti D, Schlich M, Pini E, et al. Impact of nanosizing on dermal delivery and antioxidant activity of quercetin nanocrystals. *J Drug Deliv Sci Technol.* 2020;**55**:101482. <https://doi.org/10.1016/j.jddst.2019.101482>.
- Kakran M, Shegokar R, Sahoo NG, Shaal LA, Li L, Muller RH. Fabrication of quercetin nanocrystals: comparison of different methods. *Eur J Pharm Biopharm.* 2012;**80**(1):113-21. [PubMed ID: 21896330]. <https://doi.org/10.1016/j.ejpb.2011.08.006>.
- Jain S, Patel N, Lin S. Solubility and dissolution enhancement strategies: current understanding and recent trends. *Drug Dev Ind Pharm.* 2015;**41**(6):875-87. [PubMed ID: 25342479]. <https://doi.org/10.3109/03639045.2014.971027>.
- Chogale MM, Ghodake VN, Patravale VB. Performance Parameters and Characterizations of Nanocrystals: A Brief Review. *Pharmaceutics.* 2016;**8**(3). [PubMed ID: 27589788]. [PubMed Central ID: PMC5039445]. <https://doi.org/10.3390/pharmaceutics8030026>.
- Peltonen L, Hirvonen J. Pharmaceutical nanocrystals by nanomilling: critical process parameters, particle fracturing and stabilization methods. *J Pharm Pharmacol.* 2010;**62**(11):1569-79. [PubMed ID: 21039542]. <https://doi.org/10.1111/j.2042-7158.2010.01022.x>.
- Bodratti AM, Alexandridis P. Formulation of Poloxamers for Drug Delivery. *J Funct Biomater.* 2018;**9**(1). [PubMed ID: 29346330]. [PubMed Central ID: PMC5872097]. <https://doi.org/10.3390/jfb9010011>.
- Lee J, Choi JY, Park CH. Characteristics of polymers enabling nano-comminution of water-insoluble drugs. *Int J Pharm.* 2008;**355**(1-2):328-36. [PubMed ID: 18261866]. <https://doi.org/10.1016/j.ijpharm.2007.12.032>.
- Guo Y, Luo J, Tan S, Otieno BO, Zhang Z. The applications of Vitamin E TPGS in drug delivery. *Eur J Pharm Sci.* 2013;**49**(2):175-86. [PubMed ID: 23485439]. <https://doi.org/10.1016/j.ejps.2013.02.006>.
- Li M, Alvarez P, Bilgili E. A microhydrodynamic rationale for selection of bead size in preparation of drug nanosuspensions via wet stirred media milling. *Int J Pharm.* 2017;**524**(1-2):178-92. [PubMed ID: 28380391]. <https://doi.org/10.1016/j.ijpharm.2017.04.001>.
- Wang Y, Zheng Y, Zhang L, Wang Q, Zhang D. Stability of nanosuspensions in drug delivery. *J Control Release.* 2013;**172**(3):1126-41. [PubMed ID: 23954372]. <https://doi.org/10.1016/j.jconrel.2013.08.006>.
- Verma S, Kumar S, Gokhale R, Burgess DJ. Physical stability of nanosuspensions: investigation of the role of stabilizers on Ost-

- wald ripening. *Int J Pharm.* 2011;**406**(1-2):145–52. [PubMed ID: 21185926]. <https://doi.org/10.1016/j.ijpharm.2010.12.027>.
32. Ghosh I, Schenck D, Bose S, Liu F, Motto M. Identification of critical process parameters and its interplay with nanosuspension formulation prepared by top down media milling technology—a QbD perspective. *Pharm Dev Technol.* 2013;**18**(3):719–29. [PubMed ID: 23061898]. <https://doi.org/10.3109/10837450.2012.723720>.
 33. Cerdeira AM, Mazzotti M, Gander B. Miconazole nanosuspensions: Influence of formulation variables on particle size reduction and physical stability. *Int J Pharm.* 2010;**396**(1-2):210–8. [PubMed ID: 20600732]. <https://doi.org/10.1016/j.ijpharm.2010.06.020>.
 34. Alshora D, Ibrahim M, Elzayat E, Almeanazel OT, Alanazi F. Defining the process parameters affecting the fabrication of rosuvastatin calcium nanoparticles by planetary ball mill. *Int J Nanomedicine.* 2019;**14**:4625–36. [PubMed ID: 31303752]. [PubMed Central ID: PMC6603996]. <https://doi.org/10.2147/IJN.S207301>.
 35. Liu P, Rong X, Laru J, van Veen B, Kiesvaara J, Hirvonen J, et al. Nanosuspensions of poorly soluble drugs: preparation and development by wet milling. *Int J Pharm.* 2011;**411**(1-2):215–22. [PubMed ID: 21458552]. <https://doi.org/10.1016/j.ijpharm.2011.03.050>.
 36. Shen C, Shen B, Liu X, Yuan H. Nanosuspensions based gel as delivery system of nitrofurazone for enhanced dermal bioavailability. *J Drug Deliv Sci Technol.* 2018;**43**:1–11. <https://doi.org/10.1016/j.jddst.2017.09.012>.
 37. Fonte P, Reis S, Sarmiento B. Facts and evidences on the lyophilization of polymeric nanoparticles for drug delivery. *J Control Release.* 2016;**225**:75–86. [PubMed ID: 26805517]. <https://doi.org/10.1016/j.jconrel.2016.01.034>.
 38. Kumar S, Gokhale R, Burgess DJ. Sugars as bulking agents to prevent nano-crystal aggregation during spray or freeze-drying. *Int J Pharm.* 2014;**471**(1-2):303–11. [PubMed ID: 24939612]. <https://doi.org/10.1016/j.ijpharm.2014.05.060>.
 39. Van Eerdenbrugh B, Van den Mooter G, Augustijns P. Top-down production of drug nanocrystals: nanosuspension stabilization, miniaturization and transformation into solid products. *Int J Pharm.* 2008;**364**(1):64–75. [PubMed ID: 18721869]. <https://doi.org/10.1016/j.ijpharm.2008.07.023>.
 40. Dengale SJ, Hussien SS, Krishna BS, Musmade PB, Gautham Shenoy G, Bhat K. Fabrication, solid state characterization and bioavailability assessment of stable binary amorphous phases of Ritonavir with Quercetin. *Eur J Pharm Biopharm.* 2015;**89**:329–38. [PubMed ID: 25542681]. <https://doi.org/10.1016/j.ejpb.2014.12.025>.
 41. Garcia-Casas I, Montes A, Pereyra C, Martinez de la Ossa EJ. Generation of quercetin/cellulose acetate phthalate systems for delivery by supercritical antisolvent process. *Eur J Pharm Sci.* 2017;**100**:79–86. [PubMed ID: 28087355]. <https://doi.org/10.1016/j.ejps.2017.01.010>.
 42. Liu J, Wang X, Yong H, Kan J, Zhang N, Jin C. Preparation, characterization, digestibility and antioxidant activity of quercetin grafted Cynanchum auriculatum starch. *Int J Biol Macromol.* 2018;**114**:130–6. [PubMed ID: 29572138]. <https://doi.org/10.1016/j.ijbiomac.2018.03.101>.
 43. Liu T, Muller RH, Moschwitz JP. Effect of drug physico-chemical properties on the efficiency of top-down process and characterization of nanosuspension. *Expert Opin Drug Deliv.* 2015;**12**(11):1741–54. [PubMed ID: 26098043]. <https://doi.org/10.1517/17425247.2015.1057566>.
 44. Nagarwal RC, Kumar R, Dhanawat M, Das N, Pandit JK. Nanocrystal technology in the delivery of poorly soluble drugs: an overview. *Curr Drug Deliv.* 2011;**8**(4):398–406. [PubMed ID: 21453258]. <https://doi.org/10.2174/156720111795767988>.
 45. Lai F, Sinico C, Ennas G, Marongiu F, Marongiu G, Fadda AM. Diclofenac nanosuspensions: influence of preparation procedure and crystal form on drug dissolution behaviour. *Int J Pharm.* 2009;**373**(1-2):124–32. [PubMed ID: 19429297]. <https://doi.org/10.1016/j.ijpharm.2009.01.024>.